JMEPEG (2020) 29:3494–3501
https://doi.org/10.1007/s11665-020-04635-x

1059-9495/$19.00

A Comparative Study on Cooling Performance of Hot Oil and Molten Salt Quench Media for Industrial Heat Treatment

K.M. Pranesh Rao and K. Narayan Prabhu

(Submitted November 14, 2019; in revised form January 18, 2020; published online February 11, 2020)

The present work presents a comprehensive comparative study on the cooling performance of hot oil and molten 54%KNO_3-7%$NaNO_3$-39%$NaNO_2$ eutectic mixture quench media. The study was conducted using a cylindrical Inconel probe of 12.5 mm diameter and 60 mm length. Cooling curves at different locations in the probe were acquired and were subsequently used to calculate spatially dependent transient heat flux at the metal/quenchant interface. The heat extraction mechanism in hot oil and $NaNO_2$ eutectic mixture was found to be different. Heat transfer occurred in two stages, namely boiling stage and convective cooling stage during quenching in molten $NaNO_2$ eutectic mixture. In the case of hot oil, apart from these two stages, third stage of cooling, namely vapor blanket stage, was observed. A detailed study was conducted to compare the magnitude and uniformity of heat extraction during each stage of quenching. Molten salt offered a higher cooling rate and more spatial uniform cooling as compared to that obtained in hot oil quench medium. The non-uniformity in surface temperature during boiling stage in Inconel probe was ten times lower in molten salt medium as compared to that observed in the hot oil medium. However, the non-uniformity in surface temperature during convective cooling stage in both the media were comparable. Based on the distribution of characteristic cooling time (t_{85}) calculated in quenched Inconel probe, higher and uniform hardness distribution is predicted in steel parts quenched in molten $NaNO_2$ eutectic mixture media as compared to that in hot oil.

Keywords cooling mechanism, heat treatment, molten salt, oil, quench uniformity

1. Introduction

Quench hardening heat treatment is often used to enhance the hardness and toughness of steel parts. Conventional quench hardening (liquid immersion quench hardening) process involves direct immersion of austenitized steel part in a vaporizable quenchant. This is the most commonly used technique to quench-hardenable steels and other metal. The cooling rate can be significantly controlled by changing the liquid quenchant, temperature of quenchant and agitation rate. Water, brine, oil and water-soluble polymer are widely used media for conventional quench hardening of steel parts (Ref 1).

Figure 1 shows the three stages of heat removal during quenching in vaporizable conventional liquid media, namely vapor blanket stage, nucleate boiling stage and convective cooling stage (Ref 2).

- *Vapor blanket stage* This stage is also referred to as film boiling stage. This is the first stage of quench heat extraction which occurs when the supply of heat from the surface of the quenched part is significantly higher than the amount of heat needed to vaporize the liquid quenchant. The rate of heat transfer is low during this stage as the vapor envelope acts as an insulator, and cooling occurs by radiation from part surface and conduction through the vapor film. The vapor film on the part surface breaks when the surface temperature reduces to Liedenfrost/rewetting temperature.
- The process of liquid quenchant coming in contact with the surface of the part by rupturing vapor blanket is called rewetting. Variation in the wall temperature, resulting from part geometry, surface depositions, oxide layers, immersion, pressure deviations and locally differing immersion periods, leads to locally confined rewetting. The local wetting results in simultaneous existence of all the three stages of cooling, i.e., vapor blanket, nucleate boiling and convection stages on the surface of the part during quenching. The vapor blanket stage thus results in non-uniform heat extraction at the metal/quenchant interface.
- *Nucleate boiling stage* This stage begins after rewetting of the quenched part surface. The liquid quench medium in contact with the quenched part surface boils, and a number of small bubbles are formed on the surface of the part. The evaporation of the fluid and the gravity-driven upward movement of the vapor bubble cause extremely strong convection heat transfer. This results in high heat extraction rates during this stage.

This article is an invited submission to JMEP selected from presentations at the 30th Heat Treating Society Conference and Exposition held October 15-17, 2019, in Detroit, Michigan, and has been expanded from the original presentation.

K.M. Pranesh Rao and **K. Narayan Prabhu**, Department of Metallurgical and Materials Engineering, National Institute of Technology Karnataka, Surathkal, Srinivasnagar 575 025, India. Contact e-mails: praneshraokm@gmail.com and prabhukn_2002@yahoo.co.in.

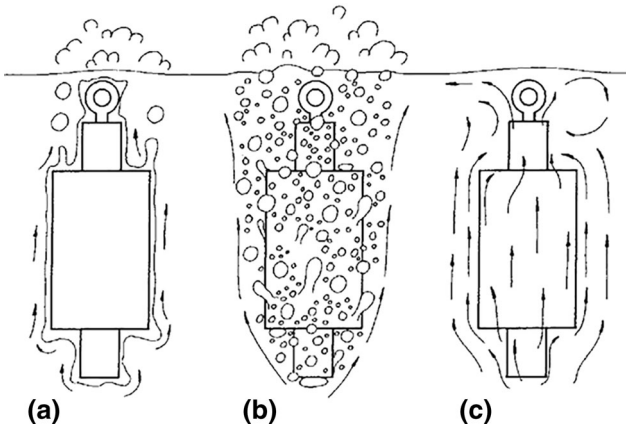

Fig. 1 Stages of quench heat extraction: (a) vapor blanket stage, (b) nucleate boiling stage, (c) convective cooling stage [2]

- *Convective cooling stage* This stage begins when the temperature of the metal surface is reduced below the boiling point of the quenchant. The quenchant exists in single phase, i.e., liquid thermo-migration takes place through heat conduction and convection. The heat extraction rate is very low compared to preceding stages.

Conventional quench hardening involves rapid cooling of austenitized steel part in a quench media maintained at room temperature. Rapid cooling of steel part to room temperature ensures the transformation of austenite to martensite by avoiding high-temperature diffusion-based transformation of austenite to ferrite, cementite or pearlite. Rapid cooling results in establishment of large thermal gradients in the steel part. Transformation stresses develop in the steel part due to volumetric expansion associated with transformation of austenite to martensite. Thermal and transformational stresses combine and appear in the form of distortion, residual stress and cracks in quench-hardened steel parts (Ref 3). Distortion, residual stress and cracking are the defects observed in steel parts subjected to conventional quench hardening heat treatment. In conventional liquid quench media, the large variation of heat transfer along the suraface of the quenched steel part increaeses the risk of quench defects in the part.

Austempering and martempering heat treatments are industrial quench hardening processes which are widely used to harden steel parts with minimum distortion, residual stress and cracking. Austempering and martempering require high-temperature quench media which can operate in the temperature range of 150-600 °C. These high-temperature quench media are expected to cool the steel part from austenitizing temperature to quench bath temperature rapidly enough to avoid transformation of austenite to ferrite, cementite and pearlite (Ref 4).

Molten salts, molten metals and hot oils (martempering oils) are widely used industrial quench media for martempering steels. The performance of molten metal and molten salt baths as quenchants do not differ greatly. Thermal diffusivity of molten salts is very low as compared to that of molten metals (Ref 5). The viscosity of molten salt bath is much lower compared to molten metal bath. The change in viscosity of molten salt quench media over a wide temperature range is not very significant. Lower viscosity eases the motion of the quenchant during agitation and hence increases the cooling performance of the quenchant.

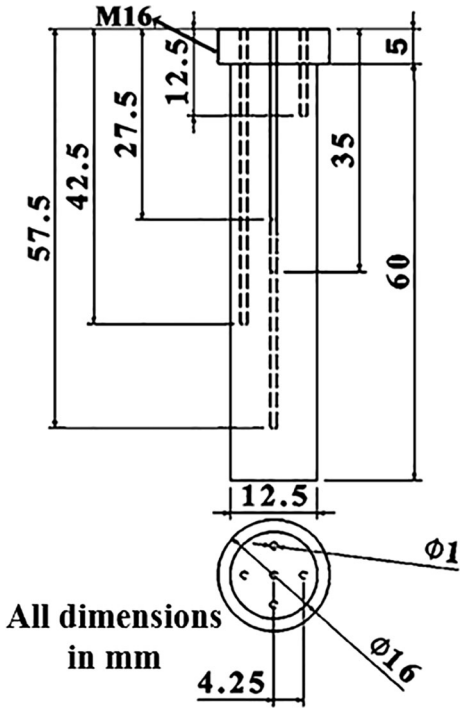

Fig. 2 Dimensions of Inconel probe

There are two main categories of quenching salts: nitrate/nitrite based and chloride based, having working ranges of 150-595 °C and 425-705 °C, respectively. Hydroxide- and carbonate-based salts are not recommended for quenching or austenitizing, because these materials adversely affect the surface corrosion susceptibility (Ref 6).

Mineral-based hot oil medium also known as martempering oil is used when the required operating bath temperature is below 250 °C. Molten eutectic mixture comprising 54%KNO_3-7%$NaNO_3$-39%$NaNO_2$ ($NaNO_2$ eutectic mixture) has a melting point of 140 °C and is used as a quench media to heat-treat steel parts where operating quench bath temperature is between 150 and 300 °C. The importance of choosing proper quench medium is emphasized in the work by Canan.et.al, which showed that characteristic temperature and hysteresis in a Cu-based quaternary shape memory alloy can be controlled by selecting a proper quench medium (Ref 7).

The present work deals with the comparison of the cooling performance of $NaNO_2$ eutectic mixture and mineral-based hot oil at a bath temperature of 150 °C.

2. Experimental Details

Figure 2 shows the dimensions of Inconel probe used for quenching experiments. Inconel cylindrical probe of 60 mm height and 12.5 mm diameter was used to perform quenching experiments. ISO 9950 recommends the use of Inconel probe 600 to characterize the cooling performance of quench media. Oxidized Inconel 600 is the preferred material for characterizing cooling media as it does not undergo transformation and distortion during quenching and ensures repeatable cooling curves. M16 thread was provided at the top of the Inconel probe. Five holes of 1 mm diameter were EDM-drilled in the

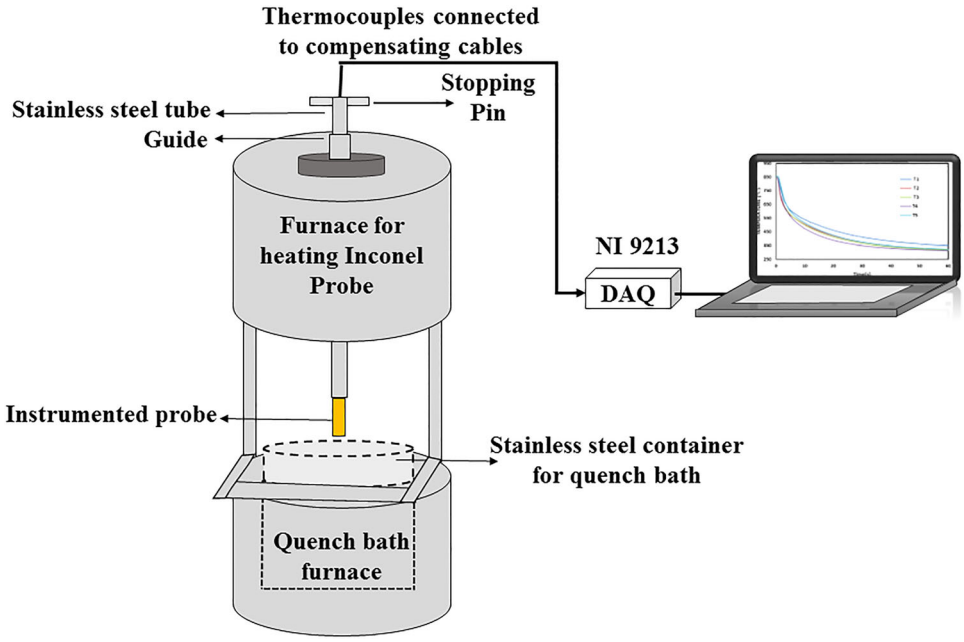

Fig. 3 Schematic of the experimental setup

probe. One hole was drilled at center to a depth of 30 mm and 4 holes drilled at 2 mm from the surface of the probe (radial distance of 4.25 mm from the center) to depths of 7.5, 22.5, 37.5 and 52.5 mm. These depths are exclusive of the 5-mm threaded section at the top of the probe. The surface of the probe was oxidized by repatedly quenching the probe from 860 °C in mineral oil maintained at room temperature. Uniform oxidation of the probe surface is necessary for obtaining repeatable cooling curve.

2.1 Quenching Experiment

Five K-type Inconel sheathed 1-mm -wide and 1-m-long thermocouples were inserted into the 1-mm EDM-drilled holes in the Inconel probe. The thermocouples were inserted through a 750-mm-long stainless-steel tube. The Inconel probe instrumented with thermocouples was fastened to the stainless-steel tube.

The schematic of experimental setup is shown in Fig. 3. Stainless-steel tube-instrumented probe arrangement was transferred to a vertical tubular furnace. The thermocouples were connected to the NI-9213 data logger via compensating cables. During quenching, temperature data at different locations in the Inconel probe were recorded at an interval of 0.1 s in the computer. Two liters of hot oil and molten KNO_3-$NaNO_3$-$NaNO_2$ eutectic media were heated in a stainless-steel container and maintained at 150 °C in a quench bath furnace. Quench bath furnace was placed below the vertical tubular furnace. The instrumented Inconel probe–stainless-steel arrangement was heated to a temperature of 860 °C. The stainless-steel tube was lowered through a guide and quenched into the quench medium.

2.2 Inverse Heat Transfer Model

Inverse heat transfer model was used to calculate spatially dependent transient heat flux at the metal/quenchant interface.

Figure 4 shows the axisymmetric model of the Inconel probe used to calculate spatially dependent transient heat flux at the metal/quenchant interface (Γ_4). The inverse problem was

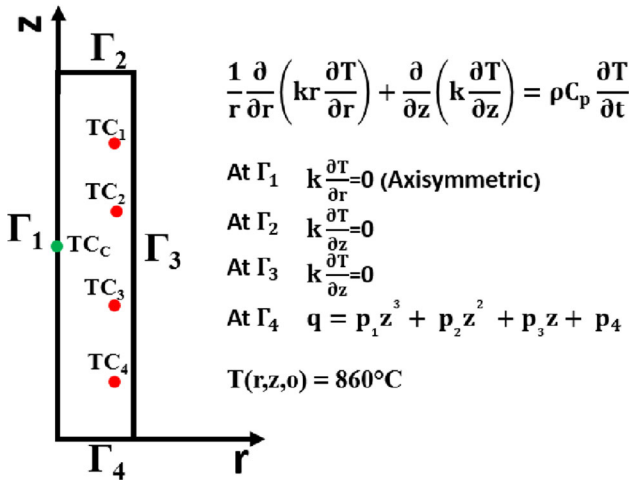

Fig. 4 Axisymmetric model of the Inconel probe used for inverse modeling

solved by minimizing the sum of square error function 'S' described in Eq 1:

$$S_{\text{ts}}=\sum_{i=1}^{n}\sum_{j=1}^{m}\left(Y_{i,\text{ts}+j-1}-T(P_{\text{ts}})_{i,\text{ts}+j-1}\right)^2 \quad \text{(Eq 1)}$$

where Y_i and T_i are the measured and calculated values of temperature at thermocouple locations at time step (ts). n is the number of thermocouples and m is number of future time steps. In the present work, the value of m and n was selected to be 4. As shown in Eq 2, P_{ts} is the vector representation of cubic parameters:

$$P_{\text{ts}}=[p_{1_{\text{ts}}},p_{2_{\text{ts}}},p_{3_{\text{ts}}},p_{4_{\text{ts}}}]. \quad \text{(Eq 2)}$$

Conjugate gradient method was used to calculate parameters p_1, p_2, p_3 and p_4 at each time step. The detailed explanation of

Table 1 Thermo-physical properties of Inconel used for inverse calculations (Ref 9)

T, °C	*k*, W/mK	C_p, J/kgK	ρ, kg/m^3
200	16	491	8340
250	16.9	…	…
300	17.8	509	8300
350	18.7	…	…
400	19.7	522	8270
450	20.7	…	…
500	21.7	533	8230
550	…	591	8190
600	25.9	597	8150
650	…	597	8100
700	30.1	611	8060

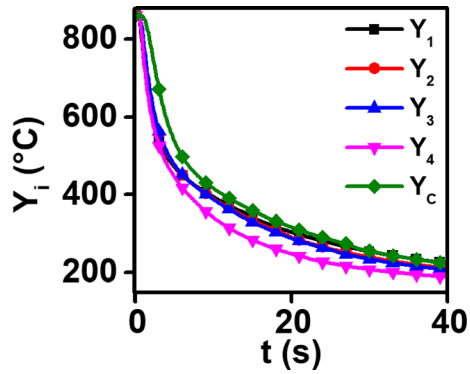

Fig. 5 Temperature measured at various locations (Y_i) versus time (t) in the *Inconel* probe quenched in $NaNO_2$ eutectic mixture maintained at 150 °C

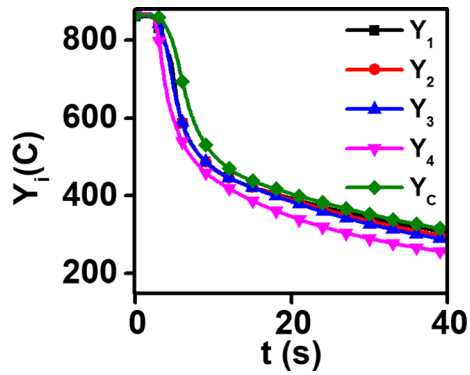

Fig. 6 Temperature measured at various locations (Y_i) versus time (t) in Inconel probe quenched in hot oil mixture maintained at 150 °C

the inverse algorithm based on conjugate gradient method used in this work is given in Ref 8:

$$q(z,t) = p_1(t)z^3 + p_2(t)z^2 + p_3(t)z + p_4(t). \quad \text{(Eq 3)}$$

The direct heat transfer problem which is a part of inverse algorithm was solved using finite element method. The axisymmetric model of the probe shown in Fig. 4 was divided into 6000 square elements of dimension 0.25 × 0.25 mm.

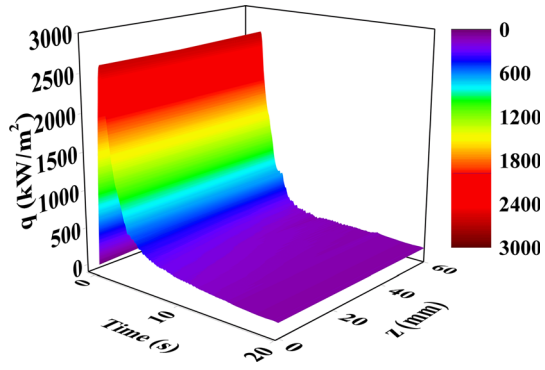

Fig. 7 Spatially dependent transient heat flux calculated for Inconel probe quenched in $NaNO_2$ eutectic mixture maintained at 150 °C

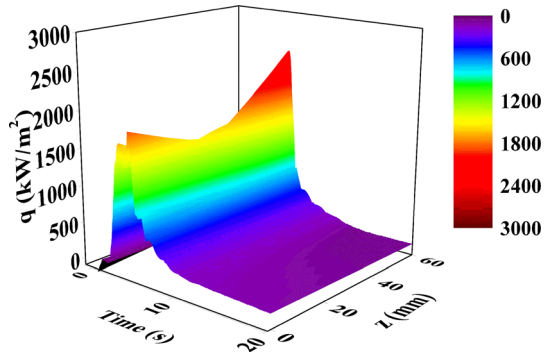

Fig. 8 Spatially dependent transient heat flux (q) calculated for Inconel probe quenched in hot oil maintained at 150 °C

Table 1 gives the thermo-physical properties of Inconel used in inverse calculations (Ref 6).

3. Results and Discussion

Figure 5 and 6 shows the cooling curves obtained for Inconel probe quenched in molten $NaNO_2$ eutectic mixtures and hot oil media maintained at 150 °C. Y_1, Y_2, Y_3, Y_4 and Y_C are the temperatures measured at locations TC_1, TC_2, TC_3, TC_4 and TC_C, respectively.

3.1 Spatially Dependent Transient Heat Flux

The measured temperature at thermocouple locations TC_1, TC_2, TC_3 and TC_4 was used to calculate spatially dependent transient quench heat flux. Figure 7 and 8 shows the spatially dependent transient heat flux calculated for $NaNO_2$ eutectic mixture and hot oil, respectively. The measured temperature at thermocouple location TC_C was not used for inverse calculation.

3.2 Validation of Inverse-Calculated Heat Flux

Figure 9 and 10 shows the transient variation of absolute %error between calculated and measured values of temperatures at all thermocouple locations during quenching of Inconel probe in hot oil and molten $NaNO_2$ eutectic mixture quench media maintained at 150 °C. The values of %error indicate the

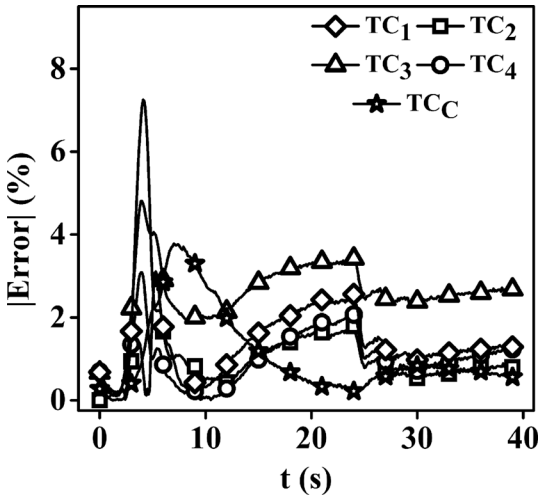

Fig. 9 %Error between measured and calculated values of temperatures versus time (t) during quenching in the Inconel probe in hot oil maintained at 150 °C

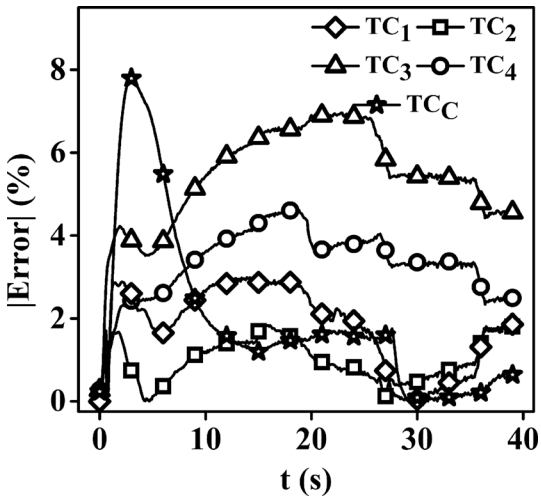

Fig. 10 %Error between measured and calculated values of temperatures during quenching in the Inconel probe $NaNO_2$ eutectic maintained at 150 °C

accuracy of spatially dependent transient quench heat flux calculated using inverse algorithm.

3.3 Heat Extraction Mechanism

Equation 4 and 5 were used to calculate average quench heat flux (q_{Avg}) and average surface temperature (T_{Avg}), respectively. The spatial integration of integration of the inverse-calculated heat flux was performed using trapezoidal method with step size of 0.25 mm. Figure 11 and 12 shows the q_{Avg} vs. T_{Avg} plots calculated for quenching of Inconel probe in $NaNO_2$ eutectic mixture and hot oil quench media maintained at 150 °C:

$$q_{\mathrm{Avg}}(t) = \frac{1}{l}\int_0^l q(t,z)\mathrm{d}z l = 60 \text{ mm} \qquad \text{(Eq 4)}$$

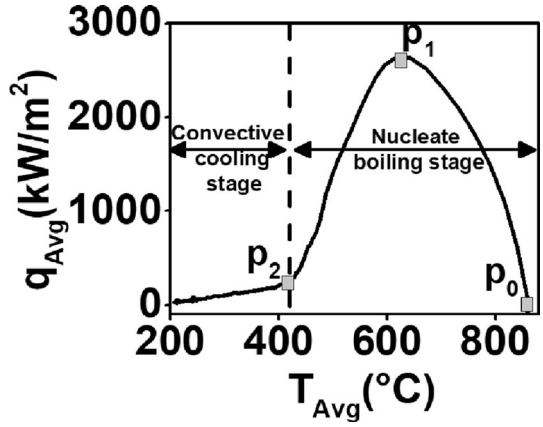

Fig. 11 Heat extraction mechanism illustrated using q_{avg} plotted as a function of average surface temperature (T_{avg}) for Inconel probe quenched in $NaNO_2$ eutectic mixture maintained at 150 °C

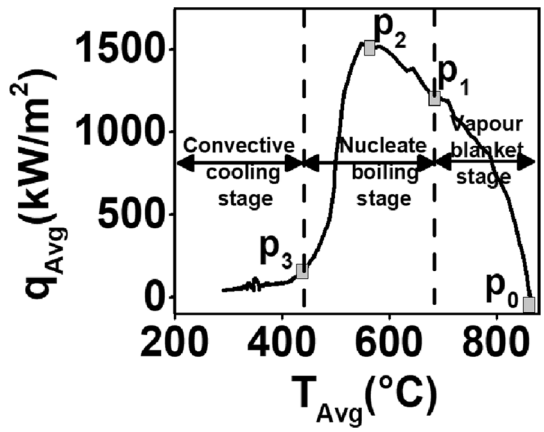

Fig. 12 Heat extraction mechanism illustrated using q_{avg} plotted as a function of average surface temperature (T_{avg}) for Inconel probe quenched in hot oil maintained at 150 °C

$$T_{\mathrm{Avg}}(t) = \frac{1}{l}\int_0^l T(t, r_{\max}, z)\mathrm{d}z r_{\max} = 6.25 \text{ mm},\ l = 60 \text{ mm}. \qquad \text{(Eq 5)}$$

Heat extraction process was observed to take place in boiling and convective cooling stages during quenching of Inconel probe in the molten salt medium. Contrary to this, heat extraction process during quenching of Inconel probe in hot oil occurred in three stages, namely vapor blanket, boiling and convective cooling stages. Figure 11 and 12 shows the heat extraction mechanism during quenching of Inconel probe in molten $NaNO_2$ eutectic mixture and hot oil. Both quench media were maintained at a bath temperature of 150 °C.

Immediately after the immersion of Inconel probe at 860 °C in the hot oil, a vapor layer encapsulates the Inconel probe. This prevents the heat transfer at metal/quenchant interface, and thus, the heat is low during this stage. Vapor blanket stage occurs between points p_0 and p_1. The decrease in surface temperature destabilizes the vapor blanket, and with rupture of vapor film (at point p_1), liquid hot oil comes in contact with the surface of the probe. Heat extraction from the probe at metal/quenchant interface occurs by boiling of hot oil between points

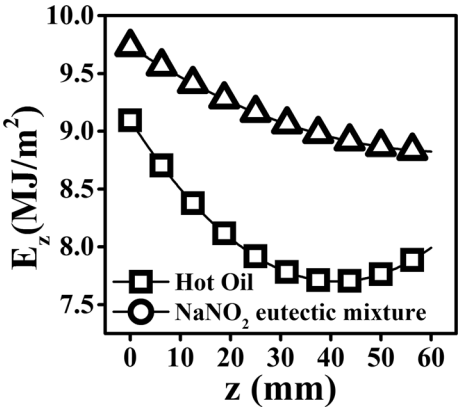

Fig. 13 Spatial distribution of energy extracted per unit area (E_z) during quenching of Inconel probe in hot oil and $NaNO_2$ eutectic mixture maintained at 150 °C

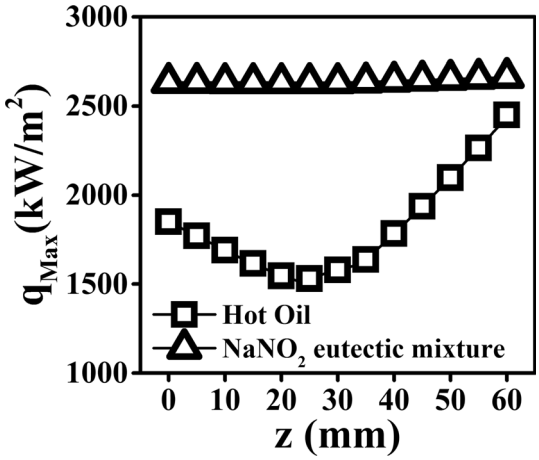

Fig. 14 Spatial distribution of peak heat flux (q_{Max}) during quenching of Inconel probe in hot oil and $NaNO_2$ eutectic mixture maintained at 150 °C

p_1 and p_2 as shown in Fig. 12. During this stage, the heat is extracted by boiling hot oil at the probe surface. The q_{Avg} thus rapidly increases to a maximum value at point p_3. Further, as T_{Avg} decreases, the average heat flux at the metal/quenchant interface also decreases and when the average surface temperature reaches point p_3, the boiling of hot oil ceases, and heat extraction occurs by convective cooling stage. During convective stage, the average surface heat flux was observed to be very low. It should be noted that all three stages of heat transfer simultaneously exist at different locations on the surface of the probe.

As shown in Fig. 11, the vapor blanket stage was absent during quenching of Inconel probe in molten salt quench media. Heat transfer occurred initially due to the boiling of the quenchant in contact with the probe surface. The average heat flux increased rapidly from point p_0 to the peak at point p_1 and then decreased to point p_2. At point 'p_2,' transition of heat transfer mechanism from boiling stage to convection stage occurs. During convective cooling stage, the heat transfer at the metal/quenchant interface occurred due to natural convection. The magnitude of average heat flux during convection stage was observed to be very low in both the cases. As observed from Fig. 11 and 12, the magnitude of heat extraction in Inconel probe quenched in hot oil is much lower compared to that observed in the molten salt medium.

Martempering oil has a flash point of 260 °C. Molten $NaNO_2$ eutectic medium has a very high thermal decomposition temperature of 631 °C (Ref 10). At temperatures higher than the thermal decomposition temperature, the salt mixture decomposes and gases comprising oxides of nitrogen evolve. Higher thermal decomposition temperature of the salt as compared to the lower flash point of oil is the reason for nonexistence of vapor blanket stage during quenching in $NaNO_2$ eutectic quench medium.

3.4 Non-uniformity of Heat Extraction

Non-uniform cooling of the quenched part during quenching would invariably result in microstructure variation, distortion or residual stress in the quenched part. Figure 13 and 14 shows the spatial variation of the energy removed per unit area (E_z) and peak heat flux (q_{Peak}), respectively:

$$E_z(z) = \int_0^t q(t,z)\mathrm{d}t = 40 \text{ s}. \quad \text{(Eq 6)}$$

To obtain heat energy extracted per unit area during quenching as a function of space, the quench heat flux at each node on boundary Γ_4 was integrated for first 40 s. The value of E_z was observed to be higher at the bottom portion and lower at the top portion of the quench probe. Thus, there exists a significant difference in heat transfer rates along the surface of the probe and more energy was removed in the bottom part as compared to the top part of the probe. The spatial variation of E_z observed in Inconel probe quenched in $NaNO_2$ eutectic mixture was much lower as compared to that in hot oil.

The peak heat flux during nucleate boiling stage is an important parameter which characterizes the heat transfer at the metal/quenchant interface. As shown in Fig. 14, the variation in peak heat flux along the surface was negligibly low in the case of molten $NaNO_2$ eutectic mixture medium maintained at 150 °C. The variation in values of peak heat flux along the surface of the probe was very large in the case of hot oil medium maintained at 150 °C. The values of peak heat flux were much lower in the bottom part of the probe as compared to the top part. This was attributed to the large amount of heat extraction during vapor blanket stage in the lower part of the probe.

3.5 Transient Variation of Cooling Uniformity

The surface temperature is not uniform along the surface of the probe. The difference between maximum and minimum temperatures (T_{Range}) thus defines the non-uniformity in the surface heat extraction. The range of surface temperature was used to study the cooling non-uniformity. T_{Range} was calculated at each time step. Figure 16 shows the variation of T_{Range} with T_{Avg}. The points O_1, O_2 and O_3 are the points corresponding to end of vapor blanket stage, maximum average heat flux and end of convective cooling stage, respectively. These points were plotted by extracting the values of T_{Avg} values of points p_1, p_2 and p_3 in Fig. 12. Similarly, in Fig. 15, points S_1 and S_2 represent maximum average heat flux and end of convective cooling stage, respectively, for $NaNO_2$ eutectic mixture main-

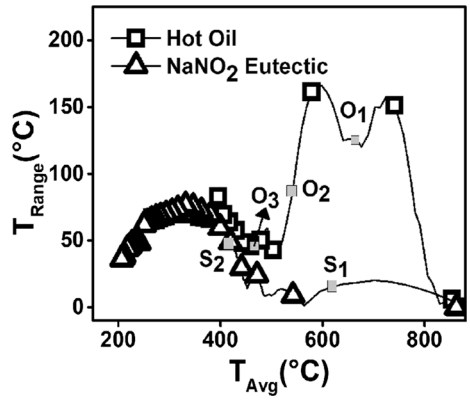

Fig. 15 Variation of T_{Range} with T_{Avg} at the metal/quenchant interface for the Inconel probe quenched in $NaNO_2$ and hot oil quench media maintained at 150 °C

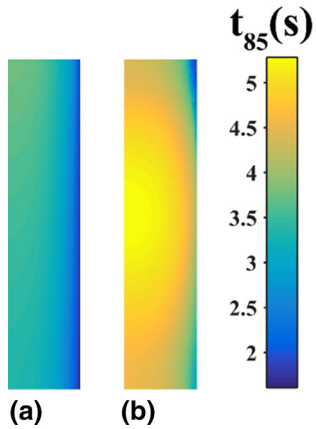

Fig. 16 Distribution of characteristic cooling time (t_{85}) values in the Inconel probe quenched in (a) $NaNO_2$ eutectic and (b) hot oil quench media maintained at 150 °C

tained at 150 °C. The T_{Avg} values of points S_1 and S_2 correspond to points p_1 and p_2 in Fig. 11.

The non-uniformity in the surface temperature reaches a maximum value first during the nucleate boing stage. Further, the non-uniformity in the surface temperature reduces to the local minima at the end of nucleate boiling and vapor blanket stages. This phenomenon was true for both hot oil and molten salt quench media. The non-uniformity in the surface temperature increased to a maximum value during convective cooling stage bust subsequently decreased. The peak non-uniformity in the surface temperature during nucleate boiling stage was higher than that observed in convective cooling stage in the case of molten salt quench medium. However, the peak non-uniformity in the surface temperature during convective cooling stage was higher than that observed in nucleate boiling stage in the case of molten salt quench medium.

The peak non-uniformity in the surface temperature during nucleate boiling and vapor blanket stages were nearly ~ 10 times higher in the case of hot oil quench medium as compared to that of the nucleate boiling stage in the molten salt medium. No significant difference in non-uniformity in the surface temperature was observed in hot oil and molten salt media during convective cooling stage.

3.6 Distribution of Characteristic Cooling Time (t_{85}) in the Inconel Probe

t_{85} is the characteristic cooling time, relevant for structure transformation for most structural steels (Ref 11). t_{85} is the time required to cool from 800 to 500 °C. The temperature distribution in Inconel probe, determined using inverse algorithm, was used to calculate t_{85} at all locations in the Inconel probe. Figure 16 shows the distribution of the t_{85} values in the Inconel probe quenched in $NaNO_2$ eutectic and hot oil quench media maintenance at 150 °C. The higher value of t_{85} values results in lower hardness in steel. If the same distribution of t_{85} values is assumed to exist in steel probe of the same dimension, the distribution of t_{85} values in Fig. 16 suggests higher hardness and uniform hardness distribution in steel probe quenched in molten $NaNO_2$ quench medium as compared to the hot oil quench medium.

4. Conclusions

- The heat extraction mechanism in hot oil was similar to conventional vaporizable quench media and occurred in three stages, namely vapor blanket, nucleate boiling and convective cooling stages. However, the heat extraction mechanism in molten KNO_3-$NaNO_2$-$NaNO_3$ eutectic mixture was observed to occur only in boiling and convective cooling stages.
- The magnitude of heat extraction rate was significantly higher in the case of molten salt media, and q_{max} was 85% higher as compared to that in the hot oil medium.
- The molten salt medium offered more uniform cooling as compared to the hot oil medium.
- The non-uniformity in surface temperature during boiling stage in Inconel probe was ten times lower in molten salt medium as compared to that observed in the hot oil medium. However, the non-uniformities in surface temperature during convective cooling stage in both the media were comparable.
- Higher and uniform hardness distribution is predicted in steel parts quenched in $NaNO_2$ eutectic mixture.

References

1. G. Ramesh and K.N. Prabhu, Wetting and Cooling Performance of Mineral Oils for Quench Heat Treatment of Steels. *ISIJ Int.*, 2014, **54**(6), p 1426–1435. https://doi.org/10.2355/isijinternational.54.1426
2. B. Lisicic, H.M. Tensi, and L.C. Canale (eds.), *Quenching Theory and Technology* (CRC Press, Boca Raton, 2010)
3. M. Narazaki, G.E. Totten, and G.M. Webster, Hardening by Reheating and Quenching, *Handbook of residual stress and deformation of steel*, G.E. Totten, M. Howes, and T. Inoue, Eds., 1st ed. (ASM International, 2002), p 248–295
4. C.E. Bates, G.E. Totten, and R.L. Brennan, Quenching, *ASM Handbook Volume 4 Heat Treating*, ASM Handbook Committee, Ed., (ASM International, Cleveland, 1991)
5. R. Sudheer and K. N. Prabhu, A Computer Aided Cooling Curve Analysis Method to Study Phase Change Materials for Thermal Energy Storage Applications, *Mater. Des.*, 2016, 95, p 198–203. https://doi.org/10.1016/j.matdes.2016.01.053

6. G.P. Dubal, Salt Bath Quenching. *Adv. Mater. Process*., 1999, **156**(6), p 23–28
7. C.A. Canbay , O. Karaduman, N. Ünlü , S.A. Baiz, and I. Ozkulb, Heat Treatment and Quenching Media Effects on the Thermodynamical, Thermoelastical and Structural Characteristics of a New Cu-Based Quaternary Shape Memory Alloy, *Composites Part B*, 2019, p 106940 (2019). https://doi.org/10.1016/j.compositesb.2019.106940
8. K.M. Pranesh Rao and K. Narayan Prabhu, Effect of Bath Temperature on Cooling Performance of Molten Eutectic $NaNO_3$-KNO_3 Quench Medium for Martempering of Steels, *Metall. Mater. Trans. A*, 2017, **48**(10), p 4895–4904. https://doi.org/10.1007/s11661-017-4267-7
9. G. Ramesh and K. Narayan Prabhu, Spatial Dependence of Heat Flux Transients and Wetting Behavior During Immersion Quenching of Inconel 600 Probe in Brine and Polymer Media, *Metall. Mater. Trans. B*, 2014, **45**(4), p 1355–1369. https://doi.org/10.1007/s11663-014-0038-7
10. A.G. Fernandez, H. Galleguillos, E. Fuentealba, and F.J. Perez, Thermal Characterization of HITEC Molten Salt for Energy Storage in Solar Linear Concentrated Technology. *J Therm Anal Calorim*., 2015, **122**(1), p 3–9. https://doi.org/10.1007/s10973-015-4715-9
11. B. Smoljan, Prediction of Mechanical Properties and Microstructure Distribution of Quenched and Tempered Steel Shaft. *J. Mater. Process. Technol*., 2006, **175**(1–3), p 393–397